Hadron–hadron interactions and nuclei production

Alessandro Balbino[1,*] **on behalf of the ALICE Collaboration**

[1]*Politecnico di Torino,*
24, Corso Duca degli Abruzzi, Turin, Italy

[1]*INFN di Torino,*
1, Via Pietro Giuria, Turin, Italy

E-mail: alessandro.balbino@polito.it

In recent years, ALICE has carried out many measurements of the production of light nuclei in pp, p–Pb and Pb–Pb collisions at different energies. Even though a clear evolution with multiplicity is measured for many key observables, the theory interpretation of this evolution is still debated. In this contribution, the measurements of the ratio between the production yields of nuclei and protons and of the coalescence parameters B_2 as a function of multiplicity are shown and compared with the predictions of the statistical hadronisation model and of the coalescence model. Moreover, the measurement of the coalescence parameter B_2 in high-multiplicity pp collisions as a function of the transverse momentum is compared with theoretical predictions that take into account both the form of the nuclear wavefunction and the dependence of the source size on the transverse momentum of the nucleons. Finally the latest measurements of the hypertriton production are reported and compared with the available theoretical models.

---

*Speaker

1. Nuclear matter production

Although at the LHC light (anti)nuclei are abundantly produced, their production mechanisms are not completely understood. Two classes of phenomenological models attempt to describe them, namely the statistical hadronisation [1] and the coalescence [2] models. According to the statistical hadronisation model (SHM), (anti)nuclei are produced at the chemical freeze-out, along with all the other hadrons. The SHM can describe the production yields ($\frac{\mathrm{d}N}{\mathrm{d}y}$) in central Pb–Pb collisions [3], including yields of nuclei, using only three parameters: temperature T, volume V and baryo-chemical potential μ_{B}. In Pb–Pb collisions, a grand canonical approach is used since the condition $VT^3 > 1$ is satisfied, where V and T are the system volume and temperature, respectively. In pp and p–Pb collisions, characterised by a smaller volume, this condition is not met and hence a canonical approach (CSM), with local conservation of quantum numbers, is used. In this work, the data are compared with the prediction of THERMAL-FIST package [4], in which baryon number, strangeness content and electric charge are exactly conserved. In the coalescence picture, nucleons that are close to each other in phase space after chemical freeze-out can form a nucleus via coalescence [2]. The main observable of the model is the coalescence parameter, defined for a nucleus of mass number A as

$$B_{\mathrm{A}} = \frac{E_{\mathrm{A}} \frac{\mathrm{d}^3 N_{\mathrm{A}}}{\mathrm{d}p_{\mathrm{A}}^3}}{\left(E_{\mathrm{p}} \frac{\mathrm{d}^3 N_{\mathrm{p}}}{\mathrm{d}p_{\mathrm{p}}^3} \right)^A}, \tag{1}$$

where the invariant spectra of the (anti)protons are evaluated at the transverse momentum of the nucleus divided by its mass number, so that $p_{\mathrm{T}}^{\mathrm{p}} = p_{\mathrm{T}}^{\mathrm{A}}/A$. Through a femtoscopic approach, the coalescence parameter estimation can be compared to a parameter-free coalescence prediction, based on the precise description of the nucleus wavefunction and on the size of the emitting source [5]. Additional information can be extracted from the study of very large and extremely loosely bound objects such as the hypertriton ($^3_\Lambda\mathrm{H}$). This nucleus has a large wave function, hence its production yield in small collision systems is extremely sensitive to the nucleosynthesis models.

2. The ratio between nucleus and proton yields

In Fig. 1, the ratio between the p_{T}-integrated yields of nuclei and protons are shown for deuterons (d/p), ^{3}He (^{3}He/p) and ^{3}H (^{3}H/p). Data are compared with the prediction of SHM obtained with the THERMAL-FIST package and with coalescence calculations [14]. The yield ratios evolve smoothly as a function of multiplicity. In both panels of Fig. 1, two regimes can be seen. In the low-multiplicity region, the yield ratios increase with multiplicity. The agreement of the multiplicity dependence of yield ratios with CSM arises because of canonical suppression, which is a consequence of conservation of baryon number [4]. In the coalescence picture, the rise at low multiplicity reflects the interplay between nucleon yield, nucleus size, and source size. Both CSM and coalescence models can qualitatively describe the ratio between the yields of nuclei and protons, except for nuclei with $A \geq 3$ in the intermediate multiplicity region. In the high-multiplicity region, the conditions for description using the grand canonical model are valid and the experimental results show no dependence on multiplicity. The coalescence models also predict a saturation of the yield ratio at high multiplicity.
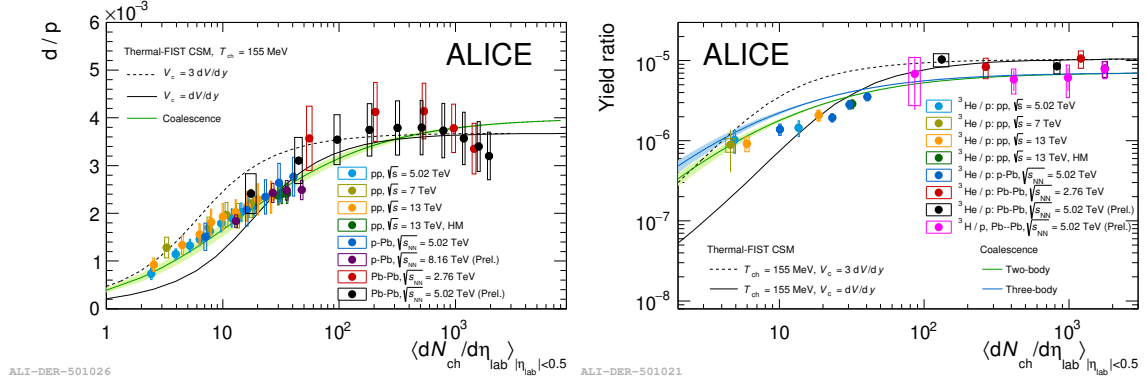
Figure 1: Ratio between the p_T-integrated yields of nuclei and protons for deuterons (d/p) [6–11] (left), ^{3}He (^{3}He/p [6, 10–13]) and ^{3}H (^{3}H/p [13]) (right). Data are compared with the predictions of the THERMAL-FIST package [4] and the coalescence model [14].
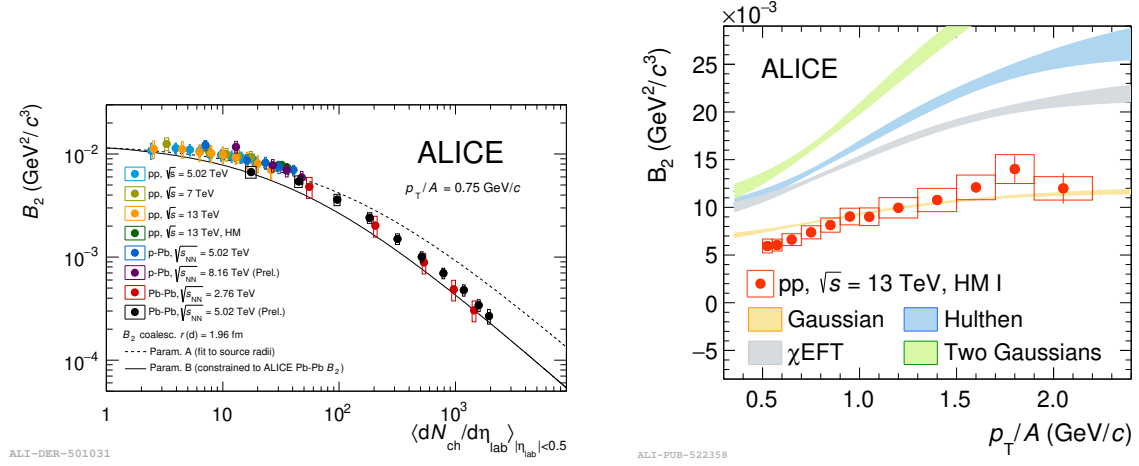

Figure 2: Left: B_2 [6–11] as a function of $\langle \frac{dN_{ch}}{d\eta} \rangle$ at p_T/A = 0.75 GeV/c. Data are compared with the predictions of two different parametrisations of the coalescence model. Right: comparison between measurements and theoretical predictions for the coalescence parameter B_2 of (anti)deuterons as a function of p_T/A [10]. Theoretical predictions are obtained by using different wave functions to describe nuclei: Gaussian (yellow), Hulthen (blue), χEFT (gray) and two Gaussians (green).

3. The coalescence parameter

The dependence of the coalescence parameter B_A on the system size can be studied by measuring for each collision system and energy the value of B_A as a function of charged particle multiplicity $\langle \frac{dN_{ch}}{d\eta} \rangle$, which is related to the system size. The left panel of Figure 2 shows B_2 as a function of $\langle \frac{dN_{ch}}{d\eta} \rangle$ at p_T/A = 0.75 GeV/c. B_2 evolves smoothly as a function of $\langle \frac{dN_{ch}}{d\eta} \rangle$, regardless of the collision system, suggesting a common production mechanism that depends only on the system size. At low multiplicity the system size is smaller than the nucleus size and B_2 slightly decreases with multiplicity. On the other hand, at high multiplicity the system size becomes larger
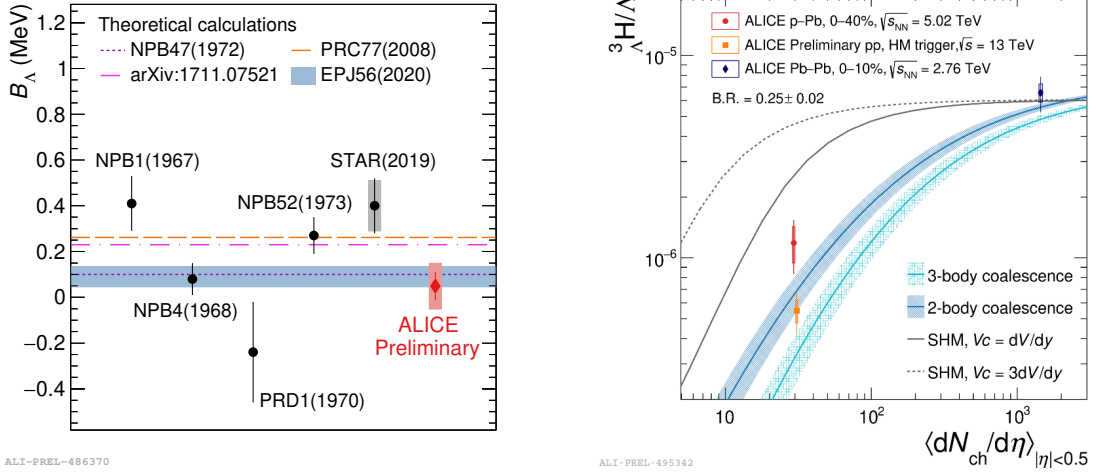
Figure 3: B_Λ measurements (left) and $^3_\Lambda H/\Lambda$ ratio (right) measurements in pp (orange), p–Pb [17] (red) and Pb–Pb collisions [18] (blue) as a function of mean charged-particle multiplicity. The theoretical predictions are also reported.

than the size of the nucleus and hence the decrease is more noticeable. Therefore, the global trend observed in the data is described by the coalescence model. Moreover, in high-multiplicity (HM) pp collisions at a center-of-mass energy $\sqrt{s} = 13$ TeV, the coalescence model is tested by combining the measurement of the production of light (anti)nuclei [10] with the precise measurement of the source radius obtained with femtoscopic techniques [15]. Using the formalism described in Ref. [5], it is possible to compare the experimentally measured coalescence parameter B_2 with parameter-free coalescence predictions, based on the measurement of the emitting source size [15] and the deuteron wave function [16]. As shown in the right panel of Fig. 2, several wave functions for deuterons are tested. The Gaussian wave function provides the best description of the currently available ALICE data, despite the Hulthen one would be favoured by low-energy scattering experiments.

4. Measurement of hypertriton production

A key observable to understand the nuclear production mechanisms in high-energy collisions is the measurement of hypertriton ($^3_\Lambda H$), a bound state of a proton, a neutron, and a Λ baryon. The left panel of Fig. 3 reports the latest measurement provided by ALICE of the $^3_\Lambda H$ binding energy (B_Λ). Since its value is measured to be small (compatible with zero), this bound state is characterized by a large radius (up to about 10 fm [19, 20]). Therefore, the size of the $^3_\Lambda H$ wave function is much larger than the hadron emission radius estimated with femtoscopic techniques in small systems (about 1–2 fm [21]). For this reason, the $^3_\Lambda H$ yield in pp and p–Pb collisions is strongly affected by its production mechanism; it is crucial to distinguish between the available nucleosynthesis models. In the right panel of Fig. 3, the $^3_\Lambda H$-to-Λ ratio measured in pp, p–Pb [17] and Pb–Pb collisions [18] are compared with the expectations of the theoretical models. The data show a good agreement with the 2-body coalescence predictions, while some tension with SHM at low charged-particle multiplicity density is observed. In particular, the SHM configuration with a correlation volume equal to three units of rapidity $V_C = 3\frac{dV}{dy}$ is excluded by more than 6σ in the low-multiplicity region.

References

[1] A. Andronic, P. Braun-Munzinger, J. Stachel and H. Stocker, *Production of light nuclei, hypernuclei and their antiparticles in relativistic nuclear collisions*, *Phys. Lett. B* **697** (2011) 203 [1010.2995].

[2] J.I. Kapusta, *Mechanisms for deuteron production in relativistic nuclear collisions*, *Phys. Rev. C* **21** (1980) 1301.

[3] ALICE collaboration, *Production of ^4He and $^4\overline{He}$ in Pb-Pb collisions at $\sqrt{s_{NN}}$ = 2.76 TeV at the LHC*, *Nucl. Phys. A* **971** (2018) 1 [1710.07531].

[4] V. Vovchenko, B. Dönigus and H. Stoecker, *Multiplicity dependence of light nuclei production at LHC energies in the canonical statistical model*, *Phys. Lett. B* **785** (2018) 171 [1808.05245].

[5] K. Blum and M. Takimoto, *Nuclear coalescence from correlation functions*, *Phys. Rev. C* **99** (2019) 044913.

[6] ALICE collaboration, *Production of light nuclei and anti-nuclei in pp and Pb-Pb collisions at energies available at the CERN Large Hadron Collider*, *Phys. Rev. C* **93** (2016) 024917 [1506.08951].

[7] ALICE collaboration, *(Anti-)deuteron production in pp collisions at $\sqrt{s}$ = 13 TeV*, *Eur. Phys. J. C* **80** (2020) 889 [2003.03184].

[8] ALICE collaboration, *Multiplicity dependence of (anti-)deuteron production in pp collisions at $\sqrt{s}$ = 7 TeV*, *Phys. Lett. B* **794** (2019) 50 [1902.09290].

[9] ALICE collaboration, *Multiplicity dependence of light (anti-)nuclei production in p-Pb collisions at $\sqrt{s_{NN}}$ = 5.02 TeV*, *Phys. Lett. B* **800** (2020) 135043 [1906.03136].

[10] ALICE collaboration, *Production of light (anti)nuclei in pp collisions at $\sqrt{s}$ = 13 TeV*, *JHEP* **01** (2022) 106 [2109.13026].

[11] ALICE collaboration, *Production of light (anti)nuclei in pp collisions at $\sqrt{s}$ = 5.02 TeV*, *Eur. Phys. J. C* **82** (2022) 289 [2112.00610].

[12] ALICE collaboration, *Production of deuterons, tritons, ^3He nuclei and their antinuclei in pp collisions at $\sqrt{s}$ = 0.9, 2.76 and 7 TeV*, *Phys. Rev. C* **97** (2018) 024615 [1709.08522].

[13] ALICE collaboration, *Production of (anti-)^3He and (anti-)^3H in p-Pb collisions at $\sqrt{s_{NN}}$ = 5.02 TeV*, *Phys. Rev. C* **101** (2020) 044906 [1910.14401].

[14] F. Bellini and A.P. Kalweit, *Testing production scenarios for (anti-)(hyper-)nuclei and exotica at energies available at the CERN Large Hadron Collider*, *Phys. Rev. C* **99** (2019) 054905 [1807.05894].

[15] ALICE collaboration, *Search for a common baryon source in high-multiplicity pp collisions at the LHC*, *Phys. Lett. B* **811** (2020) 135849 [2004.08018].

[16] F. Bellini, K. Blum, A.P. Kalweit and M. Puccio, *Examination of coalescence as the origin of nuclei in hadronic collisions*, *Phys. Rev. C* **103** (2021) 014907 [2007.01750].

[17] ALICE collaboration, *Hypertriton Production in p-Pb Collisions at $\sqrt{s_{NN}}$=5.02 TeV*, *Phys. Rev. Lett.* **128** (2022) 252003 [2107.10627].

[18] ALICE collaboration, $^{3}_{\Lambda}$H *and* $^{3}_{\Lambda}\overline{\text{H}}$ *production in Pb-Pb collisions at* $\sqrt{s_{\text{NN}}}$ = 2.76 TeV, *Phys. Lett. B* **754** (2016) 360 [1506.08453].

[19] H. Nemura, Y. Suzuki, Y. Fujiwara and C. Nakamoto, *Study of light Lambda and Lambda-Lambda hypernuclei with the stochastic variational method and effective Lambda N potentials*, *Prog. Theor. Phys.* **103** (2000) 929 [nucl-th/9912065].

[20] F. Hildenbrand and H.W. Hammer, *Lifetime of the hypertriton*, *Phys. Rev. C* **102** (2020) 064002 [2007.10122].

[21] ALICE collaboration, *p-p, p-Λ and Λ-Λ correlations studied via femtoscopy in pp reactions at* $\sqrt{s}$ = 7 TeV, *Phys. Rev. C* **99** (2019) 024001 [1805.12455].